

# Whole-Body Acoel Regeneration Is Controlled by Wnt and Bmp-Admp Signaling

Mansi Srivastava,<sup>1</sup> Kathleen L. Mazza-Curll,<sup>1</sup> Josien C. van Wolfswinkel,<sup>1</sup> and Peter W. Reddien<sup>1,\*</sup>

<sup>1</sup>Howard Hughes Medical Institute, Whitehead Institute for Biomedical Research, and Department of Biology, Massachusetts Institute of Technology, 9 Cambridge Center, Cambridge, MA 02142, USA

## Summary

Whole-body regeneration is widespread in the Metazoa, yet little is known about how underlying molecular mechanisms compare across phyla. Acoels are an enigmatic phylum of invertebrate worms that can be highly informative about many questions in bilaterian evolution, including regeneration. We developed the three-banded panther worm, *Hofstenia miamia*, as a new acoelomorph model system for molecular studies of regeneration. *Hofstenia* were readily cultured, with accessible embryos, juveniles, and adults for experimentation. We developed molecular resources and tools for *Hofstenia*, including a transcriptome and robust systemic RNAi. We report the identification of molecular mechanisms that promote whole-body regeneration in *Hofstenia*. Wnt signaling controls regeneration of the anterior-posterior axis, and Bmp-Admp signaling controls regeneration of the dorsal-ventral axis. Perturbation of these pathways resulted in regeneration-abnormal phenotypes involving axial feature duplication, such as the regeneration of two heads following Wnt perturbation or the regeneration of ventral cells in place of dorsal ones following *bmp* or *admp* RNAi. *Hofstenia* regenerative mechanisms are strikingly similar to those guiding regeneration in planarians. However, phylogenetic analyses using the *Hofstenia* transcriptome support an early branching position for acoels among bilaterians, with the last common ancestor of acoels and planarians being the ancestor of the Bilateria. Therefore, these findings identify similar whole-body regeneration mechanisms in animals separated by more than 550 million years of evolution.

## Results and Discussion

### Acoels and Regeneration

Regeneration of injured tissues is fundamental to animal biology, with degree of repair varying across species. Some animals (e.g., cnidarians, sponges, ctenophores, platyhelminths, nemertean, annelids, hemichordates, echinoderms, chordates) possess the ability to regenerate essentially any missing tissue, including entire body axes, a phenomenon often referred to as “whole-body regeneration” [1]. Whether whole-body regeneration is accomplished by similar mechanisms in diverse animals or through clade-specific processes is unknown. Acoels are little-studied bilaterally symmetric worms (phylum Acoelomorpha) that can regenerate entire bodies. We developed a novel acoel model species for molecular studies to gain insight into the mechanisms and evolution of whole-body regeneration.

There is a long-standing debate about the relationship of the Acoelomorpha to other animals. Bilaterally symmetric animals (bilaterians) are classified into protostomes and deuterostomes, and acoelomorphs were previously placed as protostomes within the phylum Platyhelminthes (flatworms) based upon morphological similarities. Some morphological studies (e.g., [2]) and several molecular studies, however, placed acoels as the earliest bilaterian lineage, i.e., a sister group to all other bilaterians [3–10]. A recent study proposed that acoelomorphs are a deuterostome clade [11]. In both of these candidate scenarios (acoels at the base of the Bilateria or within deuterostomes), comparison of regenerative mechanisms in acoels to those in protostomes could identify processes present in the last common ancestor of the Bilateria.

### *Hofstenia miamia* as a New Model System for Regeneration

We selected hofsteniids as a candidate acoel system because they were reported to regenerate [12] and are an early-diverging acoel clade with a slow rate of molecular evolution relative to other acoel lineages [13]. *Hofstenia miamia*, commonly known as three-banded panther worms (Figure 1A; see also Figure S1A available online), were collected from Walsingham Pond, Bermuda, where they live among mangrove roots [14]. *Hofstenia* have an anterior mouth, a nervous system with neuron concentration in the head, musculature, a pharynx, a dorsal sensory statocyst, and a ventral male copulatory apparatus [14] (Figures S1B–S1D). *Hofstenia* proved readily amenable to laboratory culture, producing approximately four embryos per animal per week totaling to 100 s of embryos per day in our laboratory culture. Embryos hatched in ~9 days and grew into sexually mature adults in ~8 weeks (Figure 1B). *Hofstenia* (adults and juveniles) robustly regenerated both heads and tails (Figure 1A). As reported for another acoel [15], *Hofstenia* wounds became localized ventrally and sealed within 24 hr of amputation (Figure S1E). Tails appeared within 3 days of regeneration, and a large unpigmented outgrowth (a blastema) at anterior wounds was present within 8 days of regeneration (Figure 1A). Proliferating cell numbers increased during regeneration and were largely restricted to the base of the blastema, with the blastema containing postmitotic progeny cells (Figures S1F and S1G). Changes in preexisting tissues were also evident during regeneration (Figure 1A); pigmentation stripes faded and reemerged during regeneration, suggesting respecification of positional identity in preexisting tissue occurred, a process referred to as morphallaxis in other organisms. The ease of culture, access to embryos, and capacity for whole-body regeneration make *Hofstenia* an attractive model for studies of metazoan biology and evolution.

To facilitate molecular investigations in *Hofstenia*, we generated large-scale mRNA sequencing data, resulting in 16,986 nonredundant gene contigs. We also developed protocols for studying gene expression using *in situ* hybridization, for immunohistochemistry, and for inhibiting gene function with RNAi (Figure 1C; Supplemental Experimental Procedures). RNAi was efficient, specific, and spread systemically, with dsRNA (long dsRNA from cDNA) being effectively delivered for RNAi by both injection and soaking (Figures S1H–S1K). A *piwi* gene is known to be expressed in neoblasts of the acoel *Isodiametra pulchra* [16]. We readily detected *Hofstenia*

\*Correspondence: [reddien@wi.mit.edu](mailto:reddien@wi.mit.edu)



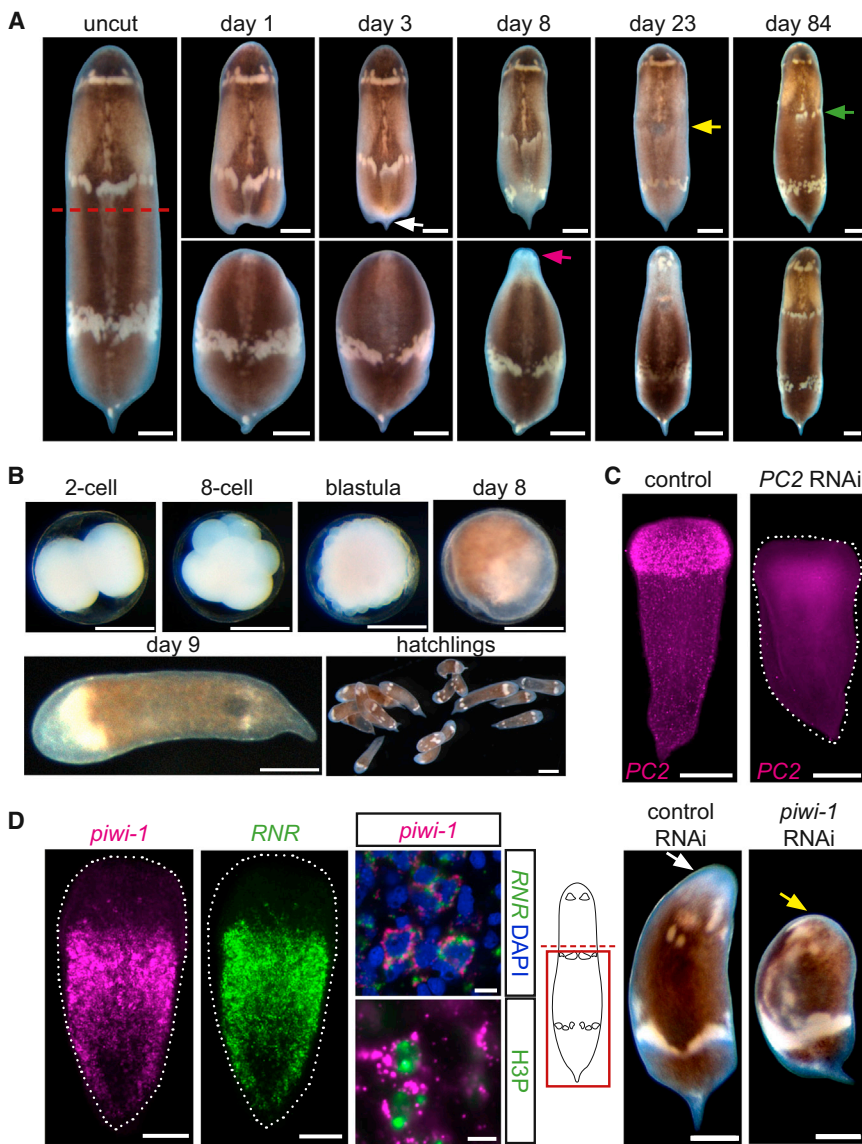


**Figure 1.** *Hofstenia miamia* as a Model Organism for Regenerative Biology

(A) An adult *Hofstenia miamia* (left) regenerated anterior and posterior tissues upon transverse amputation (dashed red line). Anterior pieces rapidly regenerated tails (white arrow), whereas posterior fragments made an unpigmented blastema (magenta arrow). The original middle white stripe faded in the anterior fragment (yellow arrow) and later was regenerated (green arrow). Scale bars represent 500  $\mu\text{m}$ .

(B) Embryonic development proceeded by duet cleavage and juvenile worms hatched 9 days after eggs were laid. Scale bars represent 200  $\mu\text{m}$ , 500  $\mu\text{m}$  for hatchlings.

(C) *prohormone convertase 2 (PC2)* mRNA was expressed in the head of control RNAi animals (21 of 23 with strong expression). *PC2* dsRNA injection abrogated *PC2* expression (22 of 26 animals showed no or weak expression). The in situ RNA probe and the dsRNA were derived from nonoverlapping gene regions. Scale bars represent 200  $\mu\text{m}$ .

(D) Mesenchymal cells excluded from the head were labeled with RNA probes for *piwi-1* and *ribonucleotide reductase (Hof-RNR)*; some of these cells were dividing (positive for the mitotic marker H3P). 100% of *RNR*<sup>+</sup> cells ( $n = 113$ ) and 93% of H3P<sup>+</sup> cells ( $n = 149$ ) were *piwi-1*<sup>+</sup>. Scale bars represent 5  $\mu\text{m}$ . Right: schematic shows amputation (red line); posterior fragments (red box) were imaged 6 days after amputation. *piwi-1* RNAi animals failed to regenerate (14 of 14; yellow arrow), whereas all control RNAi animals regenerated (15 of 15; white arrow). Scale bars represent 100  $\mu\text{m}$  (left and right) and 5  $\mu\text{m}$  (middle). Anterior is up in (A), (C), and (D). Fluorescence images are maximum-intensity projections.

*piwi*<sup>+</sup>, dividing cells (H3P<sup>+</sup>, BrdU<sup>+</sup>, *ribonucleotide reductase*<sup>+</sup>) (Figures 1D, S1L, and S1M). RNAi of *Hofstenia piwi-1* ablated regeneration and *ribonucleotide reductase*<sup>+</sup> cells, demonstrating that some Piwi proteins are required for acoel regeneration (Figures 1D and S1N). Thus, *Hofstenia* has robust and systemic RNAi, a powerful tool available for few model systems. We utilized the developed molecular tools and resources to study the mechanisms that enable *Hofstenia* whole-body regeneration.

#### Wnt Signaling Controls Regeneration of the AP Axis in *Hofstenia*

Wnt signaling is broadly used during embryonic axial patterning [17] and is required for regeneration of the anterior-posterior (AP) axis in planarians [18] and of the oral-aboral axis of cnidarians such as *Hydra* [19]. Treatment of another acoel, *Convolutri-loba retrogemma*, with a Gsk3 $\beta$  inhibitor indicated Wnt signaling might be required for acoel regeneration [20]. Therefore, we assessed the role of Wnt signaling in *Hofstenia*.

We identified genes encoding five Wnt ligands, eleven Frizzled receptors, four sFRPs (Wnt signaling antagonists),

restricted manner along the AP axis, forming oral rings, anterior domains of expression, and posterior gradients (Figures 2A and S2C).

RNAi of several Wnt pathway components resulted in striking and distinct phenotypes during regeneration. Inhibition of positive mediators of Wnt signaling (*Hof- $\beta$ -catenin-1* and *Hof-wnt-1*) resulted in failed tail regeneration (Figure 2B). In place of tails, posterior-facing mouth-like openings were frequently regenerated (10 of 20 for  *$\beta$ -catenin-1* RNAi; 18 of 20 for *wnt-1* RNAi). By contrast, RNAi of negative Wnt signaling regulators (*Hof-APC* and *Hof-axin-1*) caused formation of ectopic tail-like structures in the anterior and midbody of the regenerating animals (32 of 34 for *APC* RNAi; 13 of 20 for *axin-1* RNAi) (Figures 2B and S2D). *Hof-notum* encodes a member of a little-studied secreted hydrolase family; *notum* antagonizes Wnt signaling in planarian regeneration [21]. *Hof-notum* was expressed in the midbody and tail (*notum* in planarians is expressed at the anterior pole) and acted oppositely to Wnt signaling, with 10 of 14 *notum* RNAi animals developing anterior-facing tails. *Hof-sFRP-1* (anterior marker) and *Hof-fz-1* (posterior marker) were expressed in the ectopic

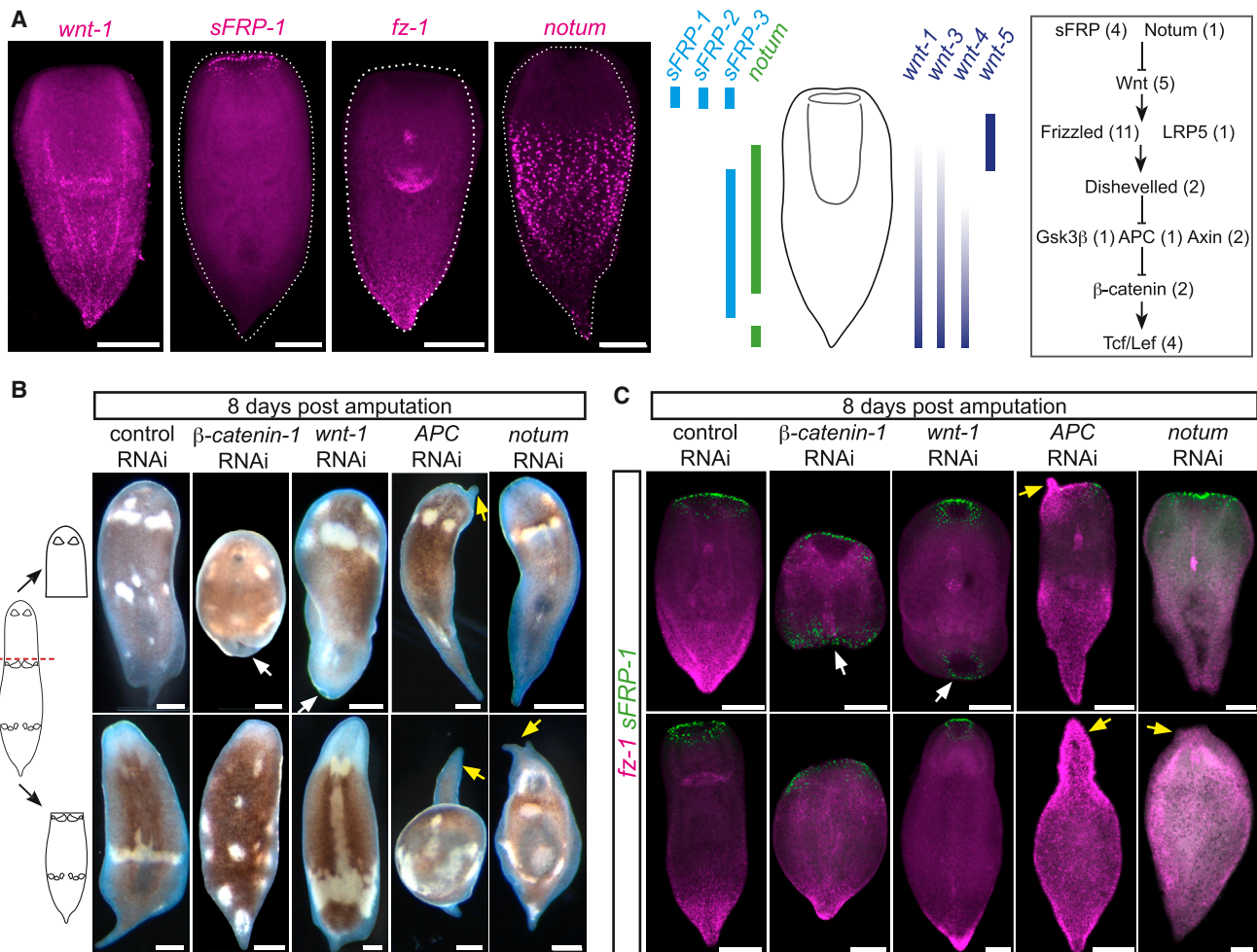


Figure 2. Wnt Signaling Is Required for Anterior-Posterior Axial Regeneration

(A) *wnt-1* was expressed in a gradient from the posterior; *sFRP-1* was expressed anteriorly around the mouth; a *frizzled* homolog (*fz-1*) was expressed in the posterior, male gonad, and the pharynx posterior; and *notum* expression was broad but absent from the head. The schematic summarizes Wnt ligand and antagonist expression (see Figure S2C). The Wnt pathway schematic (right) lists numbers of orthologs encoded in the *Hofstenia* transcriptome in parentheses.

(B) Anterior and posterior fragments were imaged 8 days after amputation. *β-catenin-1* and *wnt-1* RNAi animals failed to regenerate tails (20 of 20 each); instead, some regenerated ectopic mouth-like, posterior-facing openings (white arrows) (10 of 20 for *β-catenin-1* RNAi; 18 of 20 for *wnt-1* RNAi; 0 of 22 control RNAi animals regenerated posterior openings with 21 having tails). *APC* and *notum* RNAi posterior fragments regenerated ectopic tail-like structures (yellow arrows) in the anterior (32 of 34 for *APC* RNAi; 10 of 14 for *notum* RNAi; 0 of 31 control RNAi posterior fragments regenerated tails with 27 of 31 regenerating heads). Also unlike the control (22 of 22), anterior *APC* RNAi fragments were elongated (18 of 32) and had ectopic tail-like projections (11 of 32). Dorsal view (except the anterior *β-catenin-1* RNAi fragment) is shown.

(C) *β-catenin-1* and *wnt-1* RNAi animals expressed the anterior marker *sFRP-1* (white arrows) in the posterior in ectopic mouths (4 of 5 and 11 of 20, respectively), whereas control RNAi animals did not (26 of 26). Ectopic tails in *APC* and *notum* RNAi animals expressed the posterior marker *fz-1* (yellow arrows) (27 of 27 and 5 of 8, respectively). Posterior regenerating fragments of *notum* RNAi animals showed weak anterior expression of *sFRP-1* (7 of 8) relative to strong expression in controls (28 of 30).

Anterior is up; scale bars are 200 μm. Fluorescence images are maximum-intensity projections.

mouths and tails of RNAi animals, respectively, confirming the tissue identity defects in two-headed and two-tailed RNAi animals (Figures 2C and S2D). We screened orthologs of genes expressed in animal nervous systems and utilized identified anterior markers to determine that head-specific cell types were regenerated in the posterior of *wnt-1* RNAi animals (Figure S2E). RNAi of Wnt pathway components in unamputated animals was sufficient to lead to a transformation of the body plans of these animals, with tails disappearing in *β-catenin-1* RNAi animals and ectopic tails developing in *APC* RNAi animals (Figure S2F). We conclude that Wnt signaling is required for AP axis regeneration and homeostatic

tissue turnover, promoting posterior and inhibiting anterior tissue identity in *Hofstenia*.

#### Bmp-Admp Signaling Controls Regeneration of the DV Axis in *Hofstenia*

We next assessed the mechanisms involved in regeneration of the *Hofstenia* dorsal-ventral (DV) axis. The Bmp signaling pathway is essential for establishment of the DV axis in many bilaterian embryos [22], but its roles in whole-body animal regeneration are poorly understood. Like Bmp, another Bmp-family signaling ligand, Admp, is required for *Xenopus* DV axis patterning, with Bmp and Admp expressed on opposing sides

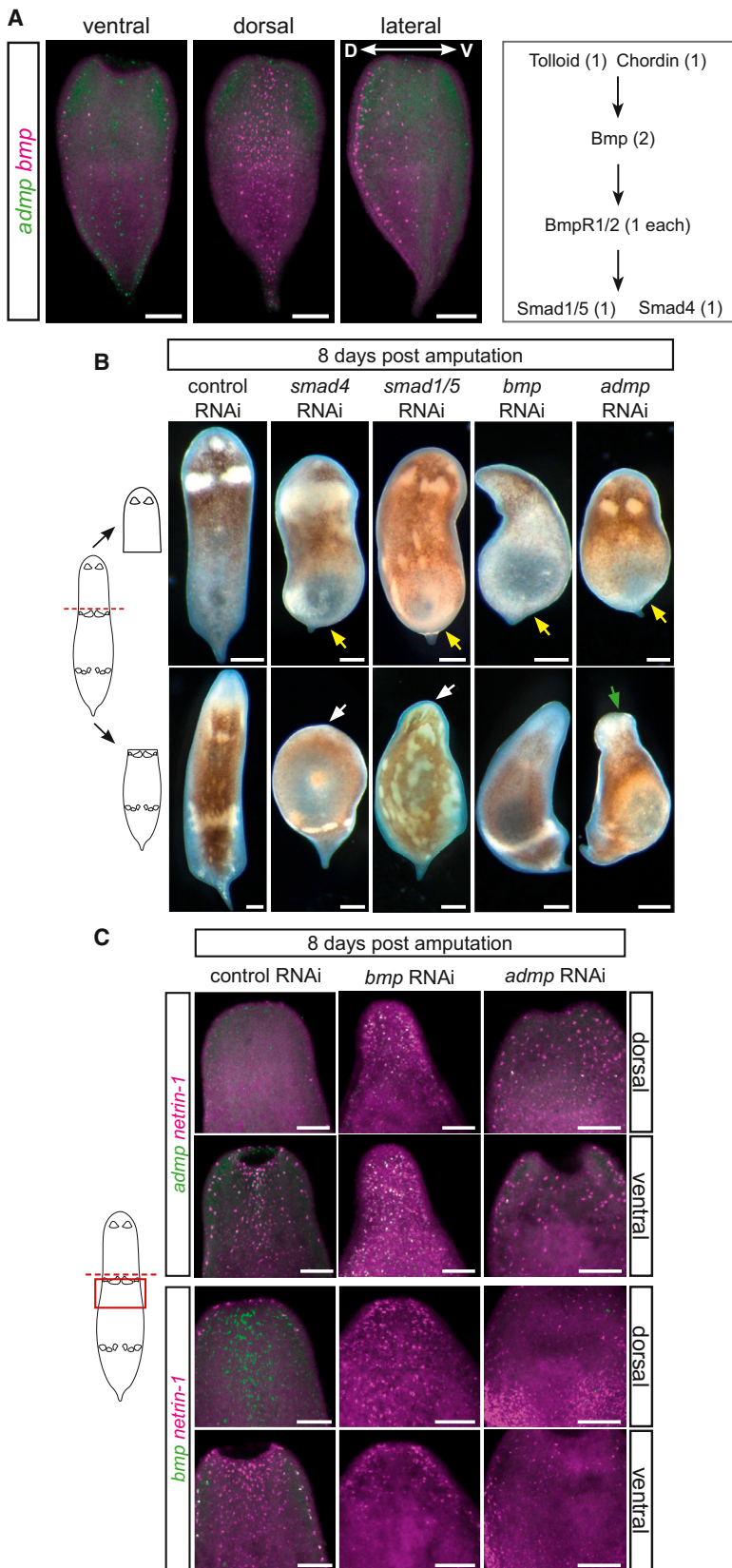


**Figure 3. Bmp Signaling Is Required for Dorsal-Ventral Polarity during Regeneration**

(A) *bmp* was expressed dorsally, whereas *admp* was expressed ventrally. In the lateral view, dorsal (D) is left and ventral (V) is right. Schematic of the Bmp pathway (right) lists numbers of orthologs from the *Hofstertia* transcriptome in parentheses.

(B) Anterior and posterior fragments were imaged 8 days after amputation. Whereas control RNAi animals regenerated normal tails (16 of 18), *smad4*, *smad1/5*, *bmp*, and *admp* RNAi animals regenerated bloated and rounded tails (21 of 21, 22 of 23, 19 of 21, and 23 of 23, respectively; yellow arrows). In contrast to normal anterior regeneration in control animals (18 of 18), posterior fragments of *smad4* (18 of 18) and *smad1/5* (17 of 23) RNAi animals failed to regenerate anterior blastemas (white arrows); *admp* RNAi animals regenerated abnormal anterior blastemas (green arrow) (17 of 23). Dorsal view is shown for all images.

(C) Schematic shows amputation (red line) and region imaged (red box). Anterior-facing wounds in *Bmp* (19 of 22) RNAi animals expressed ventral markers (*admp* and *netrin-1*; Figure S3D) dorsally, *admp* (14 of 22) RNAi animals expressed *netrin-1* dorsally, and *admp* (9 of 17) RNAi animals failed to express a dorsal marker (*bmp*). Control RNAi animals expressed dorsal (12 of 12), but not ventral (11 of 11), markers dorsally. Similar results for *smad4* and *smad1/5* RNAi animals and for posterior-facing wounds are shown in Figure S3E.

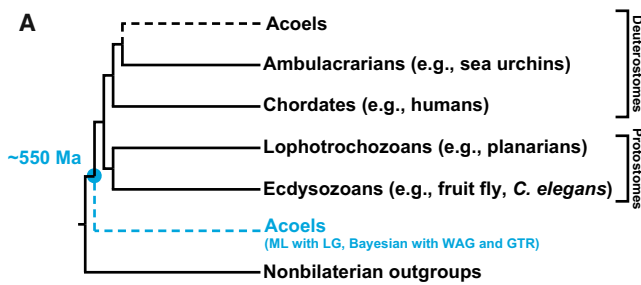
Anterior is up. Scale bars represent 100  $\mu$ m in (A) and (C) and 200  $\mu$ m in (B). Fluorescence images are maximum-intensity projections.

ligands is required for DV polarity regeneration in planarians [18, 24, 25], suggesting that spatially opposed Bmp and Admp expression might be a conserved feature of DV axis patterning.

We identified three Bmp family ligands, including orthologs of Bmp and Admp encoded in the *Hofstertia* transcriptome (Figures S3A–S3C; Supplemental Experimental Procedures). *Hof-bmp* was expressed dorsally (Figure 3A) (dorsal expression of *bmp2/4* was observed in another acoel [26]). *Hof-admp* was expressed ventrally, in a pattern mirroring *bmp* expression (Figure 3A). *bmp* and *admp* expression domains are qualitatively similar to those of their respective orthologs in planarians [18]. RNAi of *bmp*, *admp*, *Hof-smad4* (encoding a co-Smad), or *Hof-smad1/5* (encoding an R-Smad) resulted in abnormal regeneration: fragments regenerated bloated, rounded tails, and newly regenerated head and tails expressed ventral markers dorsally and lacked expression of a dorsal marker (Figures 3B, 3C, S3D, and S3E). Most *bmp* RNAi animals also failed to regenerate the dorsal statocyst (16 of 19 *bmp* RNAi versus 0 of 20 control animals). By contrast, RNAi of Wnt components did not detectably affect regeneration of the DV axis, despite AP abnormalities (Figure S3F). RNAi of *bmp* resulted in increased *admp* expression, whereas lower *admp* levels resulted in loss of *bmp* expression, suggesting a potential regulatory relationship between these

of the DV axis [23]. Admp proteins are poorly studied outside of the context of vertebrate embryos. An Admp-Bmp regulatory circuit, with similar spatially opposed expression of the two

genes in acoels. These data suggest a conserved role for an Admp-Bmp regulatory circuit for DV axis regeneration in both acoels and planarians.



**B**

**Regenerative Mechanisms Shared by Acoels and Planarians:**

- *piwi*<sup>+</sup> regenerative cells
- Wnt signaling for AP regeneration
- Bmp-Admp signaling for DV regeneration

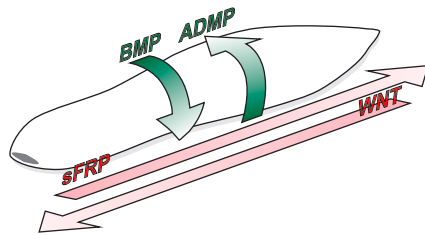


Figure 4. Model for Evolution of Regenerative Mechanisms Based on Phylogenetic Analyses

(A) A schematic tree representing two proposed positions for acoels relative to other bilaterians. Acoels as sister to other bilaterian lineages (blue line) has been proposed by others [3, 5, 6] and is supported by maximum likelihood (ML) analyses using the LG model and Bayesian analyses using the WAG and GTR models in our matrices with the *Hofstenia* transcriptome (Figure S4D; Table S1A). Acoels as a deuterostome lineage was proposed by one study [11]. Phylogenetic analyses point to short branch lengths for early divergences after the origin of bilaterians ~550 million years ago [27] (Supplemental Experimental Procedures). In both scenarios, acoels and planarians diverged early in bilaterian evolution, and therefore biological processes shared by the two can identify ancient and broadly conserved features in animal evolution.

(B) Planarians and acoels utilize similar regenerative mechanisms, involving *piwi*<sup>+</sup> regenerative cells and Wnt and Bmp-Admp signaling pathways, despite ~550 million years of independent evolution.

### Phylogenetic Analyses with the *Hofstenia* Transcriptome Support a Basal Position for Acoels within the Bilateria

The phylogenetic position of acoels is important for understanding the evolution of regeneration. We therefore evaluated this question using the *Hofstenia* transcriptome (the first phylogenetic analyses utilizing large-scale transcriptome data from an early-branching acoel species with a slow rate of molecular evolution compared to other acoels). All phylogenetic analyses reported here strongly support the conclusion that acoels are not Platyhelminthes (see Supplemental Experimental Procedures). Our analyses using maximum likelihood with the LG model and Bayesian inference with the WAG and general time reversible (GTR) models supported an early-branching position (sister to other bilaterians) for acoels (Figures 4A and S4A–S4D; Table S1), similar to several previous reports [3, 5, 6]. Whereas *Hofstenia* was consistently recovered as an early bilaterian lineage, *Xenoturbella*, an enigmatic worm lineage proposed to be closely related to acoels and deuterostomes [5, 11, 28], was an unstable branch in our analyses (Tables S2A and S2B). Hypothesis testing using maximum likelihood rejected placements of acoels in positions other than as an early-branching bilaterian, such as within deuterostomes (Tables S2C and S2D).

Bayesian inference with CAT, using expressed sequence tags from fast-evolving acoels, recently was reported to provide strong support for acoels as deuterostomes [11]. We used CAT with data sets involving the *Hofstenia* transcriptome; these analyses also strongly supported placement of acoels outside of flatworms (Figures S4E–S4H). However, this approach failed to resolve deuterostomes, with branch lengths for divergences strikingly short (Table S1A). Cladogenesis at the origin of bilaterian lineages occurred ~550 million years ago and was rapid, potentially limiting phylogenetic signal [29]. The final branching order of acoels within the lineages that emerged early in bilaterian evolution (early-branching bilaterian versus deuterostome) has therefore been a challenging problem that should continue to be further addressed, for example with genome sequencing from acoels, nemertodermatids, and xenoturbellids and with further phylogenetic tool advancement.

The early-diverging bilaterian position for *Hofstenia* obtained in our maximum-likelihood and Bayesian analyses was resistant to the removal of fast-evolving genes, distant outgroups, and genes with low phylogenetic signal (Table S3). This indicates that the early-branching bilaterian position was not readily explained as a long-branch attraction artifact. Taken together, phylogenetic analyses with the *Hofstenia* transcriptome strongly indicate that the last common ancestor shared by acoels and protostomes was the bilaterian ancestor.

### Conclusions

Given the phylogenetic data described above, any similarities in whole-body regenerative mechanisms found between *Hofstenia* and other animals would be present despite >500 million years of independent evolution. Whole-body regeneration is seen in phyla throughout the Metazoa in addition to acoels [1]. However, molecular insight into body axis regeneration exists for only a few of these organisms, including planarians, *Hydra*, and now the acoel *Hofstenia*. Our data point to striking similarity of regenerative mechanisms for two major body axes in *Hofstenia* and planarians (Wnt for the AP axis and Bmp-Admp for the DV axis; Figure 4B). Beyond bilaterians, Wnt signaling also has a prominent role in primary axis regeneration in *Hydra* [19]. These pathways also have a widely conserved role in patterning body axes during animal embryogenesis. Therefore, the similarities in regeneration between acoels and planarians can be explained in two alternative ways. First, their ancient last common ancestor (the bilaterian ancestor) could regenerate using mechanisms similar to those present in extant flatworms and acoels. Second, these pathways were independently co-opted from their roles in embryonic patterning for regeneration during lineage-specific evolution of acoels and planarians, resulting in conservation of the molecular pathways but not necessarily of the process of regeneration.

If the hypothesis of a regenerative bilaterian ancestor is correct, additional similarities in regeneration mechanisms are predicted. In addition to the similar mechanisms controlling regeneration of body axes, both organisms possess *piwi*<sup>+</sup> proliferative, mesenchymal cells that are distributed similarly and are required for regeneration; both display a combination of blastema formation and changes in preexisting tissue (morphallaxis) during regeneration; and both display constitutive expression of patterning genes in similar subepidermal domains as adults. Some of these attributes of regeneration are also observed in other animals: *piwi* is also expressed in

candidate regenerative progenitor cells in many species with whole-body regeneration, including sponges [30], cnidarians [31, 32], ctenophores [33], platyhelminthes (neoblasts) [34], annelids (in the posterior growth zone) [35], and ascidians [36], with *piwi* required for regeneration in colonial ascidians [37]. *Hofstenia* presents the tools and biology for further dissection of regeneration that will enable continued understanding of the mechanisms and evolution of whole-body regeneration. In addition to uncovering regenerative mechanisms, the developed tools, including robust systemic RNAi, place *Hofstenia* as a new and powerful model system for addressing fundamental problems in biology.

#### Experimental Procedures

For detailed methods, see [Supplemental Experimental Procedures](#).

#### Hofstenia Culturing and Fixation

Adults were collected from mangrove roots in Walsingham Pond, Bermuda. In the laboratory, they were kept in plastic boxes at 20°C in artificial sea water and fed freshly hatched brine shrimp once a week. Hatchlings were fed L-type *Brachionus* rotifers twice a week. Animals were relaxed in 1% MgCl<sub>2</sub> in sea water for 2 min and fixed in 4% paraformaldehyde in PBS with 0.1% Triton. In situ hybridization, immunostaining, and bromodeoxyuridine labeling methods are described in detail in [Supplemental Experimental Procedures](#).

#### Transcriptome Sequencing

Total RNA was collected from several stages of developing embryos and regenerating fragments of *Hofstenia*. A Roche 454 sequencing library was sequenced and assembled using Newbler. Illumina TruSeq libraries were prepared for 80 × 80 paired-end sequencing; reads were assembled using Trinity. An Illumina Tru-Seq library was also prepared for 80 × 80 paired-end sequencing from mixed regenerating stages of *Schmidtea mediterranea*.

#### Gene Identification and Cloning

Transcripts were annotated with their best BLAST hits (blastx) to human, mouse, zebrafish, *Drosophila*, and *C. elegans* proteins. Phylogenetic analyses or domain composition was used to establish orthology relationships of the proteins encoded by these transcripts to known proteins. Genes of interest were amplified by PCR from cDNA (Invitrogen SuperScript III RT kit) and cloned into the pGEM T-easy vector.

#### RNAi

dsRNA was synthesized and injected into the gut for 3 consecutive days. Animals were amputated 5 hr after the third injection and then injected again the next day. Phenotypes were monitored over the next several days, and animals were fixed 8 days after amputation. Control dsRNA was prepared from DNA sequence absent from *Hofstenia*, derived from the *C. elegans unc-22* gene.

#### Phylogenetic Analyses

Nonredundant gene sets were obtained from the *Hofstenia* and *Schmidtea* transcriptomes and from sequences of several species deposited in public databases. Three independent methods were used to cluster these sequences into orthologous gene sets. For each method, different size matrices were obtained by allowing more species to be missing per gene set. Aligned orthologous proteins were then concatenated and analyzed in a maximum-likelihood framework with the LG+G+F model and with Bayesian inference with WAG and GTR. Phylobayes was used to implement the CAT model as an alternative method to model across-site rate heterogeneity. Hypothesis testing and removal of potential sources of artifact (fast-evolving genes, genes with poor phylogenetic signal, and distant outgroups) were used to further assess the phylogeny.

#### Accession Numbers

Raw reads and corresponding assemblies for the *Hofstenia miamia* and *Schmidtea mediterranea* transcriptomes have been deposited in the NCBI Sequence Read Archive under accession numbers SRP040714 and SRP040715, respectively.

#### Supplemental Information

Supplemental Information includes four figures, three tables, and Supplemental Experimental Procedures and can be found with this article online at <http://dx.doi.org/10.1016/j.cub.2014.03.042>.

#### Acknowledgments

We would like to thank Ulf Jondelius, Wolfgang Sterrer, Stan Rachootin, Ferdinand Marletaz, Christopher Laumer, and members of the P.W.R. lab for critical input. M.S. was supported by an HHMI fellowship of the Jane Coffin Childs Memorial Fund. J.C.v.W. is supported by a Human Frontier Science Program fellowship. We acknowledge support from the Keck Foundation and the Skoltech Center for Stem Cell Research. P.W.R. is supported by HHMI and is an associate member of the Broad Institute of Harvard and MIT.

Received: November 14, 2013

Revised: February 10, 2014

Accepted: March 14, 2014

Published: April 24, 2014

#### References

1. Bely, A.E., and Nyberg, K.G. (2010). Evolution of animal regeneration: re-emergence of a field. *Trends Ecol. Evol.* 25, 161–170.
2. Haszprunar, G. (1996). Plathelminthes and Plathelminthomorpha—paraphyletic taxa. *J. Zoological Syst. Evol. Res.* 34, 41–48.
3. Ruiz-Trillo, I., Riutort, M., Littlewood, D.T., Herniou, E.A., and Bagaña, J. (1999). Acoel flatworms: earliest extant bilaterian Metazoans, not members of Platyhelminthes. *Science* 283, 1919–1923.
4. Philippe, H., Brinkmann, H., Martinez, P., Riutort, M., and Bagaña, J. (2007). Acoel flatworms are not platyhelminthes: evidence from phylogenomics. *PLoS ONE* 2, e717.
5. Hejnol, A., Obst, M., Stamatakis, A., Ott, M., Rouse, G.W., Edgecombe, G.D., Martinez, P., Bagaña, J., Bailly, X., Jondelius, U., et al. (2009). Assessing the root of bilaterian animals with scalable phylogenomic methods. *Proc. Biol. Sci.* 276, 4261–4270.
6. Mwnyi, A., Bailly, X., Bourlat, S.J., Jondelius, U., Littlewood, D.T., and Podsiadlowski, L. (2010). The phylogenetic position of Acoela as revealed by the complete mitochondrial genome of *Symsagittifera roscoffensis*. *BMC Evol. Biol.* 10, 309.
7. Telford, M.J., Lockyer, A.E., Cartwright-Finch, C., and Littlewood, D.T. (2003). Combined large and small subunit ribosomal RNA phylogenies support a basal position of the acoelomorph flatworms. *Proc. Biol. Sci.* 270, 1077–1083.
8. Ruiz-Trillo, I., Riutort, M., Fourcade, H.M., Bagaña, J., and Boore, J.L. (2004). Mitochondrial genome data support the basal position of Acoelomorpha and the polyphyly of the Platyhelminthes. *Mol. Phylogenet. Evol.* 33, 321–332.
9. Ruiz-Trillo, I., Paps, J., Loukota, M., Ribera, C., Jondelius, U., Baguna, J., and Riutort, M. (2002). A phylogenetic analysis of myosin heavy chain type II sequences corroborates that Acoela and Nemertodermatida are basal bilaterians. *Proc. Natl. Acad. Sci. USA* 99, 11246–11251.
10. Sempere, L.F., Martinez, P., Cole, C., Bagaña, J., and Peterson, K.J. (2007). Phylogenetic distribution of microRNAs supports the basal position of acoel flatworms and the polyphyly of Platyhelminthes. *Evol. Dev.* 9, 409–415.
11. Philippe, H., Brinkmann, H., Copley, R.R., Moroz, L.L., Nakano, H., Poustka, A.J., Wallberg, A., Peterson, K.J., and Telford, M.J. (2011). Acoelomorph flatworms are deuterostomes related to *Xenoturbella*. *Nature* 470, 255–258.
12. Steinbock, O. (1967). Regenerationsversuche mit *Hofstenia giselae* Steinb. (*Turbellaria* Acoela). *Roux Archiv Entwickl.* 158, 394–458.
13. Jondelius, U., Wallberg, A., Hooge, M., and Raikova, O.I. (2011). How the worm got its pharynx: phylogeny, classification and Bayesian assessment of character evolution in Acoela. *Syst. Biol.* 60, 845–871.
14. Hooge, M., Wallberg, A., Todt, C., Maloy, A., Jondelius, U., and Tyler, S. (2007). A revision of the systematics of panther worms (*Hofstenia* spp., Acoela), with notes on color variation and genetic variation within the genus. *Hydrobiologia* 592, 439–454.
15. Chiodin, M., Achatz, J.G., Wanninger, A., and Martinez, P. (2011). Molecular architecture of muscles in an acoel and its evolutionary implications. *J. Exp. Zool. B Mol. Dev. Evol.* 316, 427–439.

16. De Mulder, K., Kuaes, G., Pfister, D., Willems, M., Egger, B., Salvenmoser, W., Thaler, M., Gorny, A.K., Hrouda, M., Borgonie, G., and Ladurner, P. (2009). Characterization of the stem cell system of the acoel *Isodiametra pulchra*. *BMC Dev. Biol.* 9, 69.
17. Petersen, C.P., and Reddien, P.W. (2009). Wnt signaling and the polarity of the primary body axis. *Cell* 139, 1056–1068.
18. Reddien, P.W. (2011). Constitutive gene expression and the specification of tissue identity in adult planarian biology. *Trends Genet.* 27, 277–285.
19. Lengfeld, T., Watanabe, H., Simakov, O., Lindgens, D., Gee, L., Law, L., Schmidt, H.A., Ozbek, S., Bode, H., and Holstein, T.W. (2009). Multiple Wnts are involved in *Hydra* organizer formation and regeneration. *Dev. Biol.* 330, 186–199.
20. Sikes, J.M., and Bely, A.E. (2010). Making heads from tails: development of a reversed anterior-posterior axis during budding in an acoel. *Dev. Biol.* 338, 86–97.
21. Petersen, C.P., and Reddien, P.W. (2011). Polarized *notum* activation at wounds inhibits Wnt function to promote planarian head regeneration. *Science* 332, 852–855.
22. De Robertis, E.M., and Sasai, Y. (1996). A common plan for dorsoventral patterning in Bilateria. *Nature* 380, 37–40.
23. Reversade, B., and De Robertis, E.M. (2005). Regulation of ADMP and BMP2/4/7 at opposite embryonic poles generates a self-regulating morphogenetic field. *Cell* 123, 1147–1160.
24. Molina, M.D., Neto, A., Maeso, I., Gómez-Skarmeta, J.L., Saló, E., and Cebrià, F. (2011). Noggin and noggin-like genes control dorsoventral axis regeneration in planarians. *Curr. Biol.* 21, 300–305.
25. Gaviño, M.A., and Reddien, P.W. (2011). A Bmp/Admp regulatory circuit controls maintenance and regeneration of dorsal-ventral polarity in planarians. *Curr. Biol.* 21, 294–299.
26. Hejnal, A., and Martindale, M.Q. (2008). Acoel development indicates the independent evolution of the bilaterian mouth and anus. *Nature* 456, 382–386.
27. Peterson, K.J., Lyons, J.B., Nowak, K.S., Takacs, C.M., Wargo, M.J., and McPeck, M.A. (2004). Estimating metazoan divergence times with a molecular clock. *Proc. Natl. Acad. Sci. USA* 101, 6536–6541.
28. Huang, X., and Madan, A. (1999). CAP3: A DNA sequence assembly program. *Genome Res.* 9, 868–877.
29. Rokas, A., Krüger, D., and Carroll, S.B. (2005). Animal evolution and the molecular signature of radiations compressed in time. *Science* 310, 1933–1938.
30. Funayama, N., Nakatsukasa, M., Mohri, K., Masuda, Y., and Agata, K. (2010). *Piwi* expression in archeocytes and choanocytes in demosponges: insights into the stem cell system in demosponges. *Evol. Dev.* 12, 275–287.
31. Plickert, G., Frank, U., and Müller, W.A. (2012). *Hydractinia*, a pioneering model for stem cell biology and reprogramming somatic cells to pluripotency. *Int. J. Dev. Biol.* 56, 519–534.
32. Juliano, C.E., Reich, A., Liu, N., Götzfried, J., Zhong, M., Uman, S., Reenan, R.A., Wessel, G.M., Steele, R.E., and Lin, H. (2013). PIWI proteins and PIWI-interacting RNAs function in *Hydra* somatic stem cells. *Proc. Natl. Acad. Sci. USA* 111, 337–342.
33. Alié, A., Leclère, L., Jager, M., Dayraud, C., Chang, P., Le Guyader, H., Quéinnec, E., and Manuel, M. (2011). Somatic stem cells express *Piwi* and *Vasa* genes in an adult ctenophore: ancient association of “germline genes” with stemness. *Dev. Biol.* 350, 183–197.
34. Reddien, P.W., Oviedo, N.J., Jennings, J.R., Jenkin, J.C., and Sánchez Alvarado, A. (2005). SMEDWI-2 is a PIWI-like protein that regulates planarian stem cells. *Science* 310, 1327–1330.
35. Giani, V.C., Jr., Yamaguchi, E., Boyle, M.J., and Seaver, E.C. (2011). Somatic and germline expression of *piwi* during development and regeneration in the marine polychaete annelid *Capitella teleta*. *Evodevo* 2, 10.
36. Brown, F.D., Keeling, E.L., Le, A.D., and Swalla, B.J. (2009). Whole body regeneration in a colonial ascidian, *Botrylloides violaceus*. *J. Exp. Zool. B Mol. Dev. Evol.* 312, 885–900.
37. Rinkevich, Y., Voskoboinik, A., Rosner, A., Rabinowitz, C., Paz, G., Oren, M., Douek, J., Alfassi, G., Moiseeva, E., Ishizuka, K.J., et al. (2013). Repeated, long-term cycling of putative stem cells between niches in a basal chordate. *Dev. Cell* 24, 76–88.